

## Electrochemical hybrid additive and subtractive micro-manufacturing on a low cost desktop 3D printer

Muhammad Hazak Arshad<sup>1,2</sup>, Krishna Kumar Saxena<sup>1,2</sup>, Jun Qian<sup>1,2</sup>, Dominiek Reynaerts<sup>1,2,\*</sup>

<sup>1</sup>Micro -& Precision Engineering Group, Manufacturing Processes and Systems (MaPS) Division, Department of Mechanical Engineering, KU Leuven.

<sup>2</sup>Member Flanders Make (<https://www.flandersmake.be/nl>), Leuven, Belgium.

\*[dominiek.reynaerts@kuleuven.be](mailto:dominiek.reynaerts@kuleuven.be)

### Abstract

In this work, an electrochemical hybrid additive ( $\mu$ ECAM) and subtractive ( $\mu$ ECM) micro-manufacturing process is realized on a low-cost 3D printer platform. These electrochemical processes do not impose any thermal load on the workpiece resulting in high surface integrity with preserved microstructure and material-functionality. This opens up future application potential to carry out multiple processes in same machine e.g., repair, achieving surface roughness and dimensional tolerances, adding difficult features on machined parts as well as adding multi-materials on the same component.

The details of the hybrid setup are presented, which can alternately perform  $\mu$ ECAM and  $\mu$ ECM. This helps in performing selective micromachining and selective deposition on the same workpiece to meet functional requirements. The developed setup and proof of concept is presented through copper feature deposition with  $\mu$ ECAM along with feature machining with  $\mu$ ECM on the same stainless steel (EN-1.4301) sample. Overall, this hybrid additive and subtractive electrochemical micromanufacturing opens up avenues to produce complex and multi-material components on one machining platform and in one clamp.

**Keywords:** micro-manufacturing, micro-machining, hybrid machining, hybrid manufacturing, electrochemical additive manufacturing, electrochemical machining.

### 1. Introduction

The demand for multifunctional components and features on difficult-to-machine materials has necessitated the development of hybrid manufacturing technologies [1]. In the same line of research, the trend of laser-based hybrid additive and subtractive manufacturing has emerged to produce finished components in one machine. Despite greater flexibility and advanced applications achieved with laser-based hybrid additive and subtractive processes, the workpieces are still subjected to thermal load and hence the surface integrity is limited.

In this work, an electrochemical hybrid additive ( $\mu$ ECAM) and subtractive ( $\mu$ ECM) micro-manufacturing process is realized on a low-cost 3D printer platform. These electrochemical processes do not impose any thermal load on the workpiece resulting in high surface integrity with preserved microstructure and material-functionality. The  $\mu$ ECM [2] process can machine a wide range of electrically-conductive materials (that can be ionized and contain metal bonds) independent of hardness. Whereas,  $\mu$ ECAM [3] can locally deposit material on conductive surfaces to form functional coatings or complete parts. This helps in performing selective micromachining and selective deposition on the same workpiece to meet functional requirements. This opens up future application potential to carry out multiple processes in the same machine e.g., repair, achieving surface roughness and dimensional tolerances, adding difficult features on machined parts as well as adding multi-materials on the same component. Apart from this, some advanced applications such as adding functional elements like strain gauges on machined parts, joining of smart textiles with peripherals and fabrication of source and drain electrodes in

organic field effect transistors. Among the notable works, Li et al. [4] and Clare et al. [5] have hybridized the ECAM and ECM processes on the same setup using electrolyte jet and conductive nozzles with promising results.

In this work, the details of the hybrid setup are presented, which can alternately perform  $\mu$ ECAM and  $\mu$ ECM. The developed setup and proof of concept is presented through copper feature deposition with  $\mu$ ECAM along with feature machining with  $\mu$ ECM on the same stainless steel (EN-1.4301) sample. Overall, this hybrid additive and subtractive electrochemical micromanufacturing opens up avenues to produce complex and multi-material components on one machining platform and in one clamp.

### 2. Experimentation

#### 2.1. Experimental setup

The  $\mu$ ECAM setup [6] has been further modified on Prusa® i3 MK3S FDM 3D printer to perform both  $\mu$ ECM and  $\mu$ ECAM processes (Figure 1a). Electrolyte is pumped into the glass electrolyte container which then flows through the 400  $\mu$ m internal diameter (ID) plastic nozzle. A 350  $\mu$ m diameter copper wire is used as tool-electrode (Figure 1b) for both the processes suspended inside the nozzle. The interelectrode gap (IEG) is set by detecting the workpiece surface through the piezo-buzzer sensors (nozzle acceleration > 4 mm/s<sup>2</sup>) positioned below the manufacturing cell. A Thorlabs® MTS25-Z8 linear actuator (z stage) with a 50 nm motion resolution is superimposed on the vertical motion stage of 3D printer, for precise IEG setting in the 20-150  $\mu$ m range. A Tektronix® direct current (DC) power supply (PWS4305) provides the voltage to the circuit. A polarity switch is employed to switch between the  $\mu$ ECM and  $\mu$ ECAM processes.

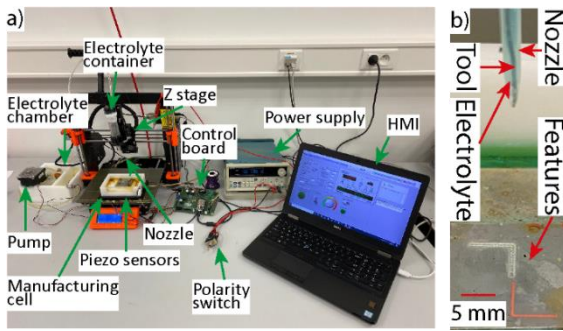


Figure 1: a) Experimental setup with major peripherals, b) A close-up view of the nozzle with wire electrode.

## 2.2. Materials and process parameters

To analyse process capability, an 'L' shaped feature of copper (Cu) was deposited on a stainless steel (S.S.) (EN-1.4301) sample and the sample itself was electrochemically machined as an inverted 'L' feature. The features were cleaned by immersion in deionized water for 10 mins. The process parameters and electrolytes used in this study are provided in Table 1 and Table 2, respectively.

Table 1: Process Parameters

| Parameters            | Value   |
|-----------------------|---|
| Voltage               | 5 V ( $\mu$ ECAM), 20 V ( $\mu$ ECM)          |
| Scan rate             | 0.1 mm/s ( $\mu$ ECAM), 0.8 mm/s ( $\mu$ ECM) |
| Scan layers           | 10  |
| IEG                   | 80 $\mu$ m                                    |
| Electrolyte flow rate | 8 mL/min                                      |

Table 2: Electrolytes

| Electrolyte                       | Properties (Conc., conductivity)        |
|-----------------------------------|---|
| aq. $\text{CuSO}_4$ ( $\mu$ ECAM) | 1 M, 40 mS/cm at 19 $^\circ\text{C}$    |
| aq. $\text{NaCl}$ ( $\mu$ ECM)    | 2.5 M, 110 mS/cm at 19 $^\circ\text{C}$ |

## 3. Results and discussion

The alternately machined and deposited features are shown in Figure 2a. Based on the used parameters, the machined S.S. sample exhibited very reduced stray pitting and the Cu deposit had minimal stray deposition. There is also no stray pitting or stray deposition at the points where scanning direction is reversed. This is possible due to the plastic nozzle around the wire which shields the current density from spreading radially outwards and is focused under the tool. The cross-sectional profile (Figure 2b) of the Cu deposit indicates that it is centred under the electrode. The cross-sectional profile of the machined feature, however, reveals a residual hill directly under the electrode where the current density is highest. This can be due to the reduced electrolyte flow in the machining zone leading to accumulation of by-products.

An important aspect is the sequence of processes and material compatibility. The results shown in this paper were achieved by doing  $\mu$ ECAM after  $\mu$ ECM. If Cu is deposited before

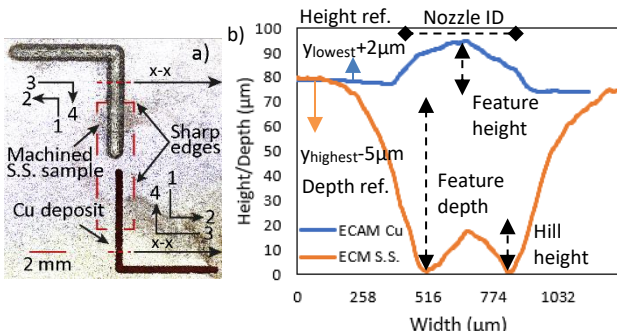


Figure 3: a) Exemplar deposited and machined features, b) Cross-sectional profiles along the section x-x in fig. (a).

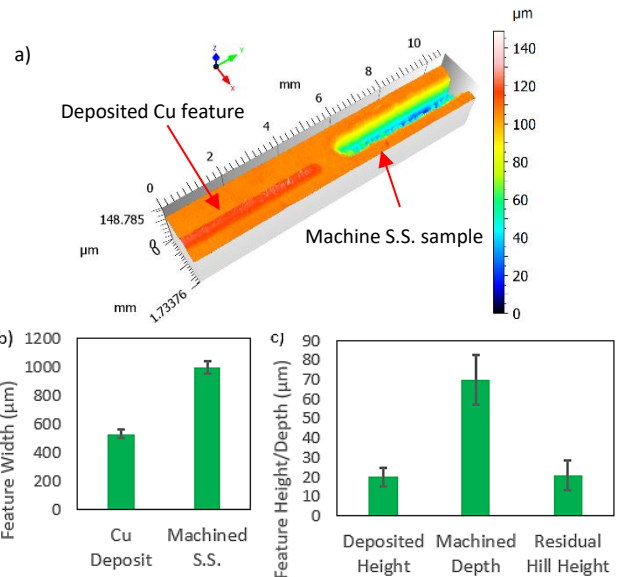


Figure 2: a) Surface scan of features at 10x objective on Sensofar® microscope, b) Feature widths, c) Feature height/depths. Error bars as standard deviation of three dimensional measurements.

S.S.  $\mu$ ECM (not shown), the more reactive Cu deposit gets partially dissolved when electrolyte spreads over the sample surface, even at locations 6 mm away from the  $\mu$ ECM machining zone. Figure 3a shows a 3D scan of the area (marked inside the red rectangle) in Figure 2a. The reference surface for height/depth measurements for  $\mu$ ECAM/ $\mu$ ECM features was defined as 2  $\mu$ m above the lowest point for  $\mu$ ECAM and 5  $\mu$ m below the highest point for  $\mu$ ECM (Figure 2b). As a consequence of the process parameters, an average height of  $(1.9 \pm 0.5) \mu\text{m}$  Cu is deposited per scan layer (Figure 3c) and the average deposit width is 33 % higher than the ID of plastic the nozzle (Figure 3b). Whereas the machined S.S. feature has significantly more (148 %) average width than the nozzle. This is due to the low electrolyte flow rate and by-products accumulation under the tool, which causes current density to spread radially around the tool, also leaving a  $(20.8 \pm 8) \mu\text{m}$  average height residual hill.

## 4. Conclusion

The characterisation of feature profiles revealed that both the  $\mu$ ECAM and  $\mu$ ECM had minimal stray deposition and pitting. The  $\mu$ ECM feature however, had significantly more (148 %) width than the plastic nozzle ID and residual hill ( $20.8 \pm 8 \mu\text{m}$  average height) as the low electrolyte flow rate (8 mL/min) resulted in by-product accumulation. The setup will be further optimized to improve  $\mu$ ECM performance by adding a separate flow line with an aim to implement the process chain hybridization technique for laser-assisted  $\mu$ ECM and  $\mu$ ECAM.

## References

- [1] G. Schuh, J. Kreysa, and S. Orilski, "Roadmap 'Hybride Produktion,'" *Zeitschrift für Wirtschaftlichen Fabrikbetr.*, vol. 104, no. 5, pp. 385–391, 2009. [Online]. Available: <https://doi.org/10.3139/104.110072>.
- [2] K. K. Saxena et al., "A review on process capabilities of electrochemical micromachining and its hybrid variants," *Int. J. Mach. Tools Manuf.*, vol. 127, no. January, pp. 28–56, 2018.
- [3] M. Kunieda, R. Katoh, and Y. Mori, "Rapid prototyping by selective electrodeposition using electrolyte jet," *CIRP Ann. - Manuf. Technol.*, vol. 47, no. 1, pp. 161–164, 1998.
- [4] T. Li et al., "In situ jet electrolyte micromachining and additive manufacturing," *Appl. Phys. Lett.*, vol. 119, no. 17, 2021.
- [5] J. Mitchell-Smith, A. Speidel, I. Bisterov, and A. T. Clare, "Electrolyte Multiplexing in Electrochemical Jet Processing," *Procedia CIRP*, vol. 68, no. April, pp. 483–487, 2018, doi: 10.1016/j.procir.2017.12.088.
- [6] M. H. Arshad et al., "Effect of electrolyte flow mode on the performance of micro-electrochemical additive manufacturing ( $\mu$ ECAM) process," in *21<sup>st</sup> INSECT Conference* (2021).